Progress In Electromagnetics Research B, Vol. 83, 61–76, 2019

Accurate Calculation of the Power Transfer and Efficiency in Resonator Arrays for Inductive Power Transfer

José Alberto[1, *], Ugo Reggiani[2], Leonardo Sandrolini[2], and Helena Albuquerque[3]

Abstract—This paper studies the power transfer characteristics of a resonator array for inductive power transfer by means of the accurate analytical solution of its circuit model. Through the mathematical inversion of a tridiagonal matrix, it is possible to obtain closed-form expressions for the current in each resonator and consequently expressions for the power transfer and efficiency of the system. The method can be applied to a resonator array powering a load at the end of the array or a receiver facing the array at any position. With the expressions obtained, it is possible not only to achieve a better understanding of the power transfer characteristics in resonator arrays but also to obtain the conditions for maximum power transfer or maximum efficiency, for several conditions and parameters of the system. A prototype of a stranded-wire resonator array powered by a resonant inverter, capable of delivering power to a load from 65 W to 90 W with efficiency values between 63% and 88%, was built in order not only to validate the expressions obtained but also to show their practical applicability and demonstrate that these arrays can be used for higher power transfer applications.

1. INTRODUCTION

Inductive power transfer (IPT) systems allow one to avoid electrical contact and transmit power even in environments with harsh conditions (water, dust or dirt) [1, 2]. In this way, they can be used in a wide number of applications (electrical vehicle charging [3], mobile devices charging [4] and powering biomedical devices [5]). In order to overcome the loss of efficiency in cases where the emitter and receiver coils are distant, arrays of resonators can be used to transfer power over longer distances [6–10]. In these arrays the first resonator is usually connected to a power source and transmits power through magnetic coupling to the other resonators of the array, which are arranged in a plane with parallel axes [9, 11–15], or alternatively, in domino configurations [7, 8, 10].

These arrays have been studied in literature using magnetoinductive wave theory [9, 15], with a representation of the array as a cascade of identical two-ports [10], or using circuit analysis [7, 8, 11]. Regarding the circuit model of a resonator array, it is also known in literature that the array can be represented by an impedance matrix which contains the impedance of each resonator and the mutual inductances between pairs of resonators as in [7–9, 12, 16, 17]. Using the inverse of this impedance matrix, it is possible to obtain the current in each resonator, which can be used to determine the power delivered to a load at the end of the array or to a receiver placed over any array resonator and consequently determine the efficiency of the system. In literature the inverse of this matrix is usually solved numerically, using specific values of circuit parameters. However, no analytical solution of this impedance matrix can be found in literature. Moreover, regarding the prototypes that use resonator arrays presented in literature, these usually use RF amplifiers as power source and deliver up to a few

Received 4 December 2018, Accepted 12 February 2019, Scheduled 19 February 2019
* Corresponding author: José Alberto (jose.alberto@isr.uc.pt).
[1] Institute of Systems and Robotics, Department of Electrical and Computer Engineering, University of Coimbra, Polo II, Coimbra 3030-290, Portugal. [2] University of Bologna, Department of Electrical, Electronic, and Information Engineering, Viale del Risorgimento 2, I-40136 Bologna, Italy. [3] Department of Mathematics of University of Coimbra, Coimbra, Portugal.

watts of power [7–9, 15]. These arrays can be used to extend the charging range of domestic electronic devices, as mobile phones or laptops, to allow the charge of more devices at the same time and, if the prototypes are further improved, could be used for electrical vehicle inductive road-charging.

In this paper, using the mathematical inversion of a generic tridiagonal matrix, closed-form expressions for the currents, power transferred and efficiency are obtained for different types of arrays of resonators. With these expressions, it is possible not only to have a better insight of the behaviour of the system, but also to obtain the conditions that guarantee maximum power transfer and/or maximum efficiency. After the description of the circuit in Section 2, the development of the expressions and some numerical examples are given in Section 3 in order to illustrate the analytical results obtained. Finally, in Section 4, with an experimental setup using a resonant inverter to feed an array with stranded wire resonators, capable of delivering up to 90 W to a load, the expressions obtained in this work are validated thus showing a practical applicability of the formulas presented.

2. DESCRIPTION OF THE CIRCUIT: CASES OF STUDY

In this section, we describe the circuit studied and present the relevant cases in order to analyse the power transmission using a resonator array. Considering an array with N identical resonators in which the first behaves as the emitter coil and is connected to an ideal sinusoidal voltage source $\hat{V}_s$ and the last one (Nth) to a termination impedance $\hat{Z}'_T$, its equivalent circuit can be represented as shown in Fig. 1. Each resonator has an impedance $\hat{Z} = R + j\omega L + 1/(j\omega C)$, being L the inductance of the resonator, R its intrinsic resistance and C the added capacitance. At the resonant angular frequency $\omega_0 = 2\pi f_0 = 1/\sqrt{LC}$, the impedance of each resonator becomes equal to its resistance ($\hat{Z} = R$). For simplicity of the circuit analysis, only the main resonant angular frequency ω_0 is considered and the frequency splitting phenomenon [16] is not considered. The mutual inductance between adjacent resonators is given by M whereas the one between non adjacent resonators is neglected, as its value is much smaller compared to M in arrays arranged in a plane with parallel axes [9, 15]. It can be calculated analytically following the procedure described in [18]. Then, the equivalent circuit can be written in matrix form as:

$$\hat{\mathbf{V}} = \hat{\mathbf{Z}}_\mathbf{m}\hat{\mathbf{I}} \tag{1}$$

with

$$\hat{\mathbf{V}} = [\hat{V}_s, 0, \ldots, 0]^T \tag{2}$$

being the current vector represented by

$$\hat{\mathbf{I}} = [\hat{I}_1, \ldots, \hat{I}_N]^T \tag{3}$$

and the matrix $\hat{\mathbf{Z}}_\mathbf{m}$ is a tridiagonal matrix:

$$\hat{\mathbf{Z}}_\mathbf{m} = \begin{bmatrix} \hat{Z} & j\omega M & \ldots & 0 \\ j\omega M & \hat{Z} & \ldots & 0 \\ \vdots & \vdots & \ddots & j\omega M \\ 0 & 0 & j\omega M & \hat{Z} + \hat{Z}'_T \end{bmatrix}. \tag{4}$$

As Eq. (4) shows, the elements of the sub-diagonals of the impedance matrix are identical and equal to $j\omega M$. Moreover, all elements of the impedance matrix main diagonal are identical and equal

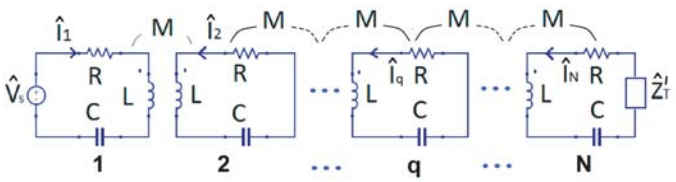

Figure 1. Equivalent circuit of an array of N resonators.

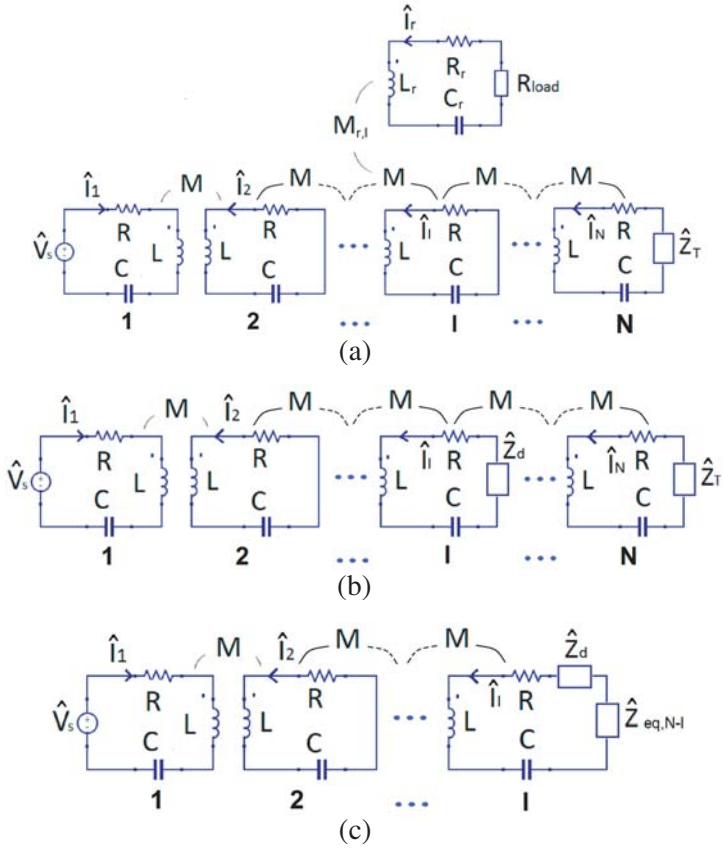

Figure 2. Circuit representations of a possible configuration of the considered resonator array: (a) receiver over the lth cell, (b) receiver represented by an impedance $\hat{Z}_d$ and (c) its equivalent circuit ($\hat{Z}'_T = \hat{Z}_d + \hat{Z}_{eq,N-l}$).

to $\hat{Z}$ except for the last one which is represented by $\hat{Z} + \hat{Z}'_T$, as in Fig. 1. In case the array is simply terminated in a load $\hat{Z}_T$, $\hat{Z}'_T = \hat{Z}_T$ represents the load. If a receiver is over the lth cell (with $N > l$) of the array, as shown in Fig. 2(a), it can be represented by an impedance $\hat{Z}_d$ (see Fig. 2(b)), which is the impedance of the receiver seen from the lth cell [9, 15], and all the resonators after the lth one ($N - l$ resonators) can be represented with an equivalent impedance $\hat{Z}_{eq,N-l}$ (see Fig. 2(c)), as in [14]. Thus, $\hat{Z}'_T = \hat{Z}_d + \hat{Z}_{eq,N-l}$ and the the matrix in Eq. (4) becomes an $l \times l$ matrix. In the particular case where the receiver is over the last cell (Nth), i.e., $l = N$, the equivalent impedance becomes $\hat{Z}_{eq,N-l} = \hat{Z}_T$.

In order to calculate the value of the current vector in Eq. (3), i.e., the currents flowing in the resonators, as $\hat{\mathbf{I}} = \hat{\mathbf{Z}}_\mathbf{m}^{-1}\hat{\mathbf{V}}$ we need to determine the inverse matrix $\hat{\mathbf{Z}}_\mathbf{m}^{-1}$. Considering Eq. (2), where only the first element is different than zero, we can obtain the values of the currents by knowing the first column of $\hat{\mathbf{Z}}_\mathbf{m}^{-1}$ only ($\hat{\mathbf{Z}}^{-1}_{\mathbf{m}(1,1)}, \ldots, \hat{\mathbf{Z}}^{-1}_{\mathbf{m}(N,1)}$). By determining the current in each resonator one can determine also the power transmitted to a given load or receiver and the efficiency of the system, as it will be shown in Section 3.

3. DETERMINATION OF THE CURRENT IN EACH RESONATOR, POWER AND EFFICIENCY

In this section, the analytical expressions of the current in each resonator, the power delivered to a load or a receiver, and the efficiency of the system and their maximum values are presented. In the examples the values $L = 12.6\,\mu\text{H}$, $C = 93.1\,\text{nF}$, $R = 0.11\,\Omega$, $M = -1.55\,\mu\text{H}$ (determined through

measurements made on the experimental setup described in Section 4) are used. Note that for the considered array layout, the mutual inductance between each pair of adjacent resonators is considered negative as in [9, 15]. The resonant frequency is $f_0 = 147\,\text{kHz}$.

3.1. Currents in the Resonators

According to the mathematical determination of the inverse of a tridiagonal matrix described in [19], we can then obtain the first column of $\hat{\mathbf{Z}}_\mathbf{m}^{-\mathbf{1}}$, that allows the expression of the current in the qth resonator to be found as:

$$\hat{I}_q = \hat{V}_s \frac{(-2j\omega M)^{q-1}\left(\left(\iota_3 + 2\hat{Z}'_T\right)\iota_3^{N-q} - \left(\iota_2 + 2\hat{Z}'_T\right)\iota_2^{N-q}\right)}{\left(\hat{Z} + \hat{Z}'_T\right)\left(\iota_3^N - \iota_2^N\right) + 2\,(\omega M)^2\left(\iota_3^{N-1} - \iota_2^{N-1}\right)} \tag{5}$$

where $\iota_2 = \hat{Z} - \sqrt{4(\omega M)^2 + \hat{Z}^2}$ and $\iota_3 = \hat{Z} + \sqrt{4(\omega M)^2 + \hat{Z}^2}$.

Equation (5) can be used to examine the distribution of currents in the resonators of an array terminated in a load. For example, with reference to Fig. 1, an array of 8 identical resonators is considered; for a given voltage source $\hat{V}_s = 1\,\text{V}$, the current magnitudes in the resonators at the resonant frequency f_0 for three different termination impedances are shown in Fig. 3. It can be noticed that when the array is perfectly terminated ($R'_T = R_{eq,\infty}$), the current magnitude decreases smoothly from the first to the last resonator. The perfectly matching impedance is the termination impedance that makes the equivalent impedance of the array constant and equal to R'_T regardless of the number of resonators; its value is $R_{eq,\infty} = (-R + \sqrt{4(\omega_0 M)^2 + R^2})/2$ [11] and for the array considered in the example $R_{eq,\infty} = 1.38\,\Omega$. If the array is terminated with a different impedance, the current magnitude oscillates from the first to the last resonator and the peaks occur on even or odd resonators, depending whether $R'_T < R_{eq,\infty}$ or $R'_T > R_{eq,\infty}$, respectively.

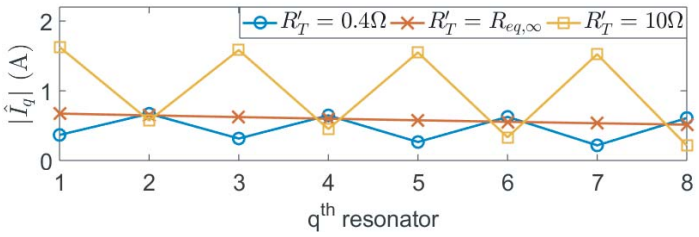

Figure 3. Magnitude of the current $\hat{I}_q$ in the qth resonator of an array of 8 resonators, for different values of R'_T ($0.4\,\Omega$, $R_{eq,\infty} = 1.38\,\Omega$ and $10\,\Omega$).

When the array is perfectly terminated we have

$$\frac{\hat{I}_{q+1}}{\hat{I}_q} = \frac{-2j\omega_0 M}{R + \sqrt{4(\omega_0 M)^2 + R^2}} \tag{6}$$

whose value is $0.9562j$ in this example (see Fig. 3). The ratio of the currents in two consecutive resonators thus depends on the electrical parameters of the array and the frequency only; it is independent on the termination impedance $R_{eq,\infty}$. For a low-loss line, i.e., $R \ll \omega_0 M$, Eq. (6) becomes equal to j, meaning that all the currents have the same magnitude and have a phase difference of $\pi/2$.

3.2. Efficiency and Power Delivered to a Load or a Receiver over the Last Cell

At the resonant frequency the efficiency (ratio of the power absorbed by R_T to the array input power) is:

$$\eta = \frac{P_{R_T}}{P_{in}} = \frac{{I_N}^2 R_T}{V_s I_1} \tag{7}$$

in which I_1, I_N and V_s are the RMS values of the currents in the first and Nth resonator and of the voltage source, respectively. Using Eq. (5) the power P_{R_T} delivered to a load R_T and the efficiency η in Eq. (7) can be written as functions of the electrical parameters of the array and the load R_T:

$$P_{R_T} = \frac{4^N V_s^2 R_T \left(\omega_0 M\right)^{2N-2} \iota_1^2}{\left[\left(R+R_T\right)\left(\iota_3^N - \iota_2^N\right) + 2\left(\omega_0 M\right)^2\left(\iota_3^{N-1} - \iota_2^{N-1}\right)\right]^2}, \tag{8}$$

$$\eta = \frac{4^{N+1} R_T \left(\omega_0 M\right)^{2N} \iota_1^2}{\left[\left(\iota_2^N\left(\iota_3 R_T - 2\left(\omega_0 M\right)^2\right) + \iota_3^N\left(2\left(\omega_0 M\right)^2 - \iota_2 R_T\right)\right)\left(\iota_1\left(\iota_2^N + \iota_3^N\right) - \left(R+2R_T\right)\left(\iota_2^N - \iota_3^N\right)\right)\right]} \tag{9}$$

where $\iota_1 = \sqrt{4(\omega M)^2 + \hat{Z}^2}$, ι_2 and ι_3 are written for $f = f_0$.

It is interesting to notice that P_{R_T} depends on V_s, too, which is the given RMS value of the voltage source that feeds the array. Thus, in the following we consider the load power for the voltage $V_s = 1\,\mathrm{V}$ indicating it, for simplicity, with the same symbol P_{R_T}.

Using Eqs. (8) and (9), the values of R_T that yield the maximum efficiency and maximum power transfer can be determined analytically by solving

$$\frac{d\eta}{dR_T} = 0, \quad \frac{dP_{R_T}}{dR_T} = 0$$

for R_T, thus obtaining

$$R_{T,\eta_{\max}} = \frac{\omega_0 |M| \sqrt{R\left(\iota_3^N - \iota_2^N\right) + \iota_1\left(\iota_2^N + \iota_3^N\right)}}{\sqrt{R\left(\iota_2^N - \iota_3^N\right) + \iota_1\left(\iota_2^N + \iota_3^N\right)}} \tag{10}$$

and

$$R_{T,P_{R_T}\max} = \frac{R\iota_2^N - \iota_1\iota_2^N - R\iota_3^N - \iota_1\iota_3^N}{2\iota_2^N - 2\iota_3^N}, \tag{11}$$

respectively. These termination impedances $R_{T,\eta_{\max}}$ and $R_{T,P_{R_T}\max}$ depend on the number of resonators N of the array, as shown in Figs. 4(a) and 4(b), where P_{R_T} and η are plotted versus R_T for different N, respectively. As regards P_{R_T} (for $V_s = 1\,\mathrm{V}$), higher or lower values of the power delivered to a load are obtained depending on whether the array has an odd or an even number of cells. In the example considered, for R_T greater than about $2\,\Omega$ higher values of P_{R_T} are obtained for arrays with an even number of cells ($N = 2$, 4, 6 and 8); conversely, when R_T is smaller than about $1\,\Omega$, higher P_{R_T} values are obtained for arrays with an odd number of cells ($N = 1$, 3, 5 and 7). Differently, Fig. 4(b) shows that for a given R_T the efficiency decreases with increasing N.

Further, by means of Eqs. (10) and (11), the following considerations can be made. The dependency of $R_{T,\eta_{\max}}$ and $R_{T,P_{R_T}\max}$ on N is clearly shown in Figs. 5(a) and 5(b); it can be noticed that both Eqs. (10) and (11) tend to the same constant value for increasing N, the latter with larger oscillations. This can be proved considering an ideal array with an infinite number of resonators, which can be approximated by a very long resonator line; from Eq. (10) we get

$$\lim_{N\to\infty} R_{T,\eta_{\max}} = \lim_{N\to\infty} R_{T,P_{R_T}\max} = \frac{R + \sqrt{4\left(\omega_0 M\right)^2 + R^2}}{2} \tag{12}$$

whose value is $1.44\,\Omega$ in both Figs. 5(a) and 5(b).

Moreover, it is interesting to note that the value given by Eq. (12) tends to $\omega_0 M$ for a low-loss line ($R \ll \omega_0 M$), which is the perfectly matching impedance of a long low-loss line according to the magnetoinductive wave theory [9, 15].

By substituting Eq. (10) in Eq. (9) and Eq. (11) in Eq. (8), the maximum efficiency of the system η and maximum power delivered to R_T for an array of N resonators with certain electrical parameters can be obtained. In order to facilitate this analysis, we can define a parameter r

$$r = R/(2\omega_0|M|). \tag{13}$$

The higher r is, the higher the losses of the resonator array are, and so r tends to zero for a low-loss line. This ratio r is simply $1/|kQ|$ that, according to the magnetoinductive wave theory, increases the

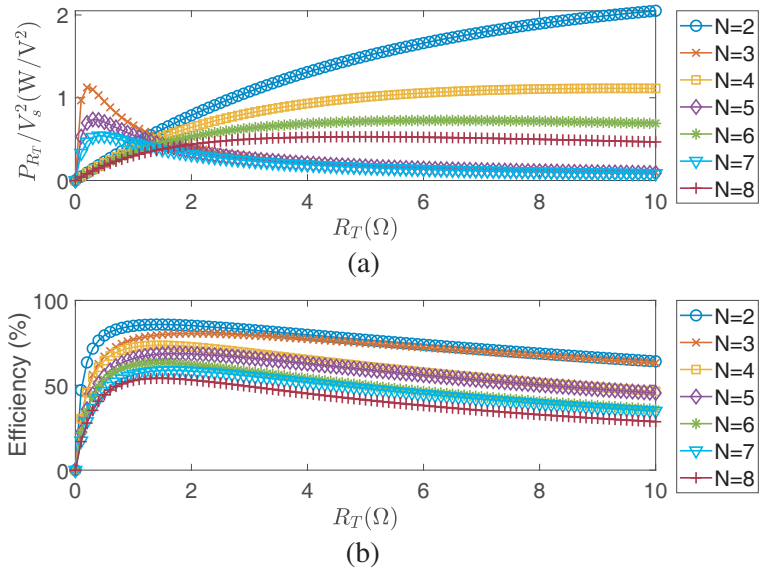

Figure 4. Values of (a) the power absorbed by R_T and (b) the efficiency (%) versus R_T for different numbers of resonators N.

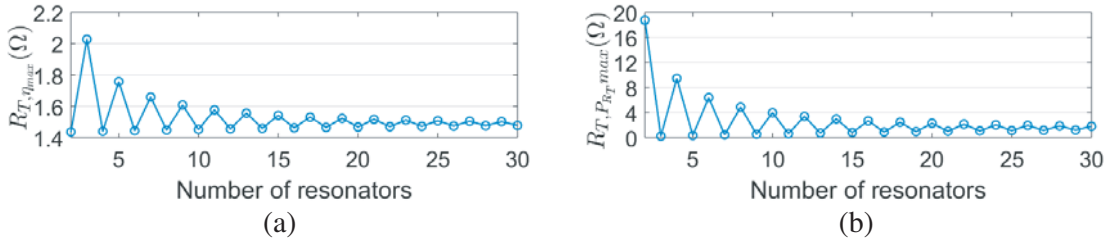

Figure 5. Values of (a) $R_T, \eta_{\max}$ versus the number of resonators N and (b) $R_T, P_{R_T\,\max}$ versus the number of resonators N.

attenuation in each cell [9, 15]. Then, for different values of r, we can plot the maximum power delivered to a load $P_{R_T,\max}$ and the maximum efficiency $\eta_{\max}$ for an array with N resonators (Figs. 6(a) and 6(b), respectively).

As expected, both $\eta_{\max}$ and $P_{R_T,\max}$ decrease with increasing r (i.e., with the decrease of $|kQ|$) due to higher losses and attenuation in the array) and the number of resonators N.

3.3. Efficiency and Power Transmitted to a Receiver R_d over the lth Cell

At the resonant frequency the efficiency (ratio of the power absorbed by R_d to the input power) is:

$$\eta_{R_d} = \frac{P_{R_d}}{P_{in}} = \frac{{I_l}^2 R_d}{V_s I_1} \tag{14}$$

where I_1, I_l, and V_s are the RMS values of the currents in the first and lth resonators and of the voltage source. Using Eq. (5), replacing N with l and $\hat{Z}'_T$ with $R_d + R_{eq,N-l}$ in Eqs. (8) and (9), we can write the power delivered to a receiver over the lth position and the efficiency as Eqs. (15) and (16).

$$P_{R_d} = \frac{4^l V_s^2 R_d (\omega_0 M)^{2l-2} \iota_1^2}{\left[\left(R + R_d + R_{eq,N-l}\right)\left(\iota_3^l - \iota_2^l\right) + 2\left(\omega_0 M\right)^2 \left(\iota_3^{l-1} - \iota_2^{l-1}\right)\right]^2} \tag{15}$$

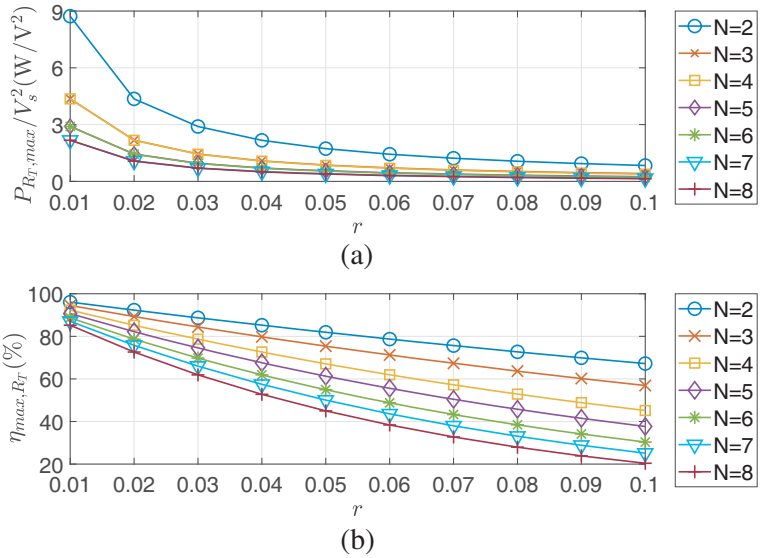

Figure 6. Values of (a) the maximum power delivered to R_T and (b) the maximum efficiency versus r for different numbers of resonators N.

$$\eta_{R_d} = \frac{4^{l+1}R_d(\omega_0 M)^{2l}\iota_1^2}{\left[\begin{array}{c}\left(\iota_1\left(\iota_2^l+\iota_3^l\right)+\left(\iota_3^l-\iota_2^l\right)\left(R+2\left(R_d+R_{eq,N-l}\right)\right)\right)\\ \left(\left(R_d+R_{eq,N-l}\right)\left(\iota_1\left(\iota_2^l+\iota_3^l\right)+R\left(\iota_2^l-\iota_3^l\right)\right)-2\left(\omega_0 M\right)^2\left(\iota_2^l-\iota_3^l\right)\right)\end{array}\right]} \tag{16}$$

Note that, for the particular situation where there is a receiver over the Nth cell and the line is terminated by R_T, we can determine the power delivered to R_d and efficiency of the system by replacing l with N and $R_{eq,N-l}$ with R_T in Eqs. (15) and (16), respectively.

With Eqs. (15) and (16) the power delivered to a receiver R_d (for $V_s = 1\,\mathrm{V}$) and the efficiency of the system can be plotted versus R_d and $R_{eq,N-l}$ and for the different positions of the receiver over the array, as shown in Figs. 7(a) and 7(b), respectively.

$$P_{R_{d(R_{eq,N-l}=R_{eq,\infty})}} = \frac{4^l V_s^2 R_d(\omega_0 M)^{2l-2}\iota_1^2}{\left[R_d\left(\iota_3^l-\iota_2^l\right)+\iota_1\iota_3^l\right]^2} \tag{17}$$

$$\eta_{R_{d(R_{eq,N-l}=R_{eq,\infty})}} = \frac{2^{2l+1}R_d\left(\omega_0 M\right)^{2l}\left(4(\omega_0 M)^2+R^2\right)}{\left[\begin{array}{c}\left(\iota_1\iota_3^l+R_d\left(\iota_3^l-\iota_2^l\right)\right)\left(-R\left(\iota_1\iota_3^l-R_d\iota_2^l+R_d\iota_3^l\right)\right)+\\ +\ \iota_1 R_d\left(\iota_2^l+\iota_3^l\right)+4\left(\omega_0 M\right)^2\iota_3^l+R^2\iota_3^l\end{array}\right]} \tag{18}$$

From Fig. 7(a) it can be observed that, similar to what observed in Fig. 4(a), P_{R_d} presents different behaviours for odd and even values of l (i.e., the receiver position). For example, considering $R_d = R_{eq} = 5\,\Omega$, P_{R_d} has the highest values when the receiver is on even positions ($l = 2$, 4, 6 and 8) and lowest values for odd positions ($l = 1$, 3, 5 and 7), for the same value of $R_{eq,N-l}$. Moreover, as can be noticed in both Figs. 7(a) and 7(b), both the power delivered to a receiver and the efficiency increase for decreasing values of $R_{eq,N-l}$. However, as shown in [11], $R_{eq,N-l}$ has an oscillating value, depending on the number of resonators after the receiver, the termination impedance of the array and the electrical parameters of the system. In order to make $R_{eq,N-l}$ constant the array must be perfectly terminated with $R_T = R_{eq,\infty}$, so that the equivalent impedance $R_{eq,N-l}$ of all the resonators after the lth one is always equal to $R_{eq,\infty}$ regardless of the number of resonators N and for any position of the receiver l (with $N \geq l$). By replacing $R_{eq,N-l}$ with $R_{eq,\infty}$ in Eqs. (15) and (16) we get Eqs. (17) and (18) that can be plotted versus R_d and for different positions of the receiver l (see Figs. 8(a) and 8(b), respectively).

As seen also in the previous case, the power delivered to a receiver has higher or lower values depending on the parity of the position of the receiver, while the efficiency decreases as the distance of

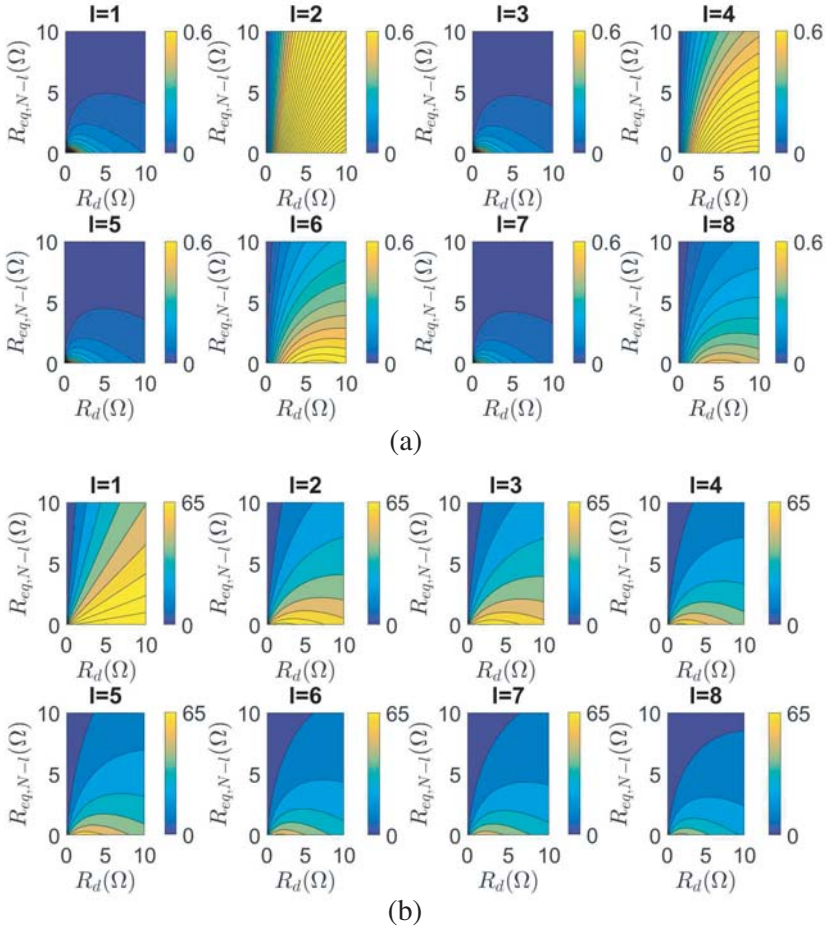

Figure 7. Values of (a) the power delivered to R_d, P_{R_d} (W), determined with Eq. (15) and (b) the efficiency (%) determined with Eq. (16) versus $R_{eq,N-l}$ and R_d and for different positions of the receiver l.

the receiver from the power source increases. Moreover, it is interesting to note that for any position of the receiver, the variation of the power delivered to it and the efficiency versus R_d is less than that in Figs. 4(a) and 4(b).

The values of R_d that guarantee the maximum efficiency, $R_{d,\eta_{R_d}\max}$, and maximum power delivered to R_d, $R_{d,P_{R_d}\max}$, can be found by solving

$$\frac{d\eta_{R_d}(R_{eq,N-l}=R_{eq,\infty})}{dR_d}=0; \quad \frac{dP_{R_d}(R_{eq,N-l}=R_{eq,\infty})}{dR_d}=0 \tag{19}$$

for R_d, thus obtaining

$$R_{d,\eta_{R_d}\max(R_{eq,N-l}=R_{eq,\infty})}=\frac{\sqrt{\iota_1^2(-\iota_2)\iota_3^{2l}}}{\sqrt{\left(\iota_3^l-\iota_2^l\right)\left(R\left(\iota_2^l-\iota_3^l\right)+\iota_1\left(\iota_2^l+\iota_3^l\right)\right)}} \tag{20}$$

and

$$R_{d,P_{R_d}\max(R_{eq,N-l}=R_{eq,\infty})}=-\frac{\iota_1\iota_3^l}{\iota_2^l-\iota_3^l}. \tag{21}$$

Equations (20) and (21) are plotted versus the position of the receiver in Figs. 9(a) and 9(b), respectively.

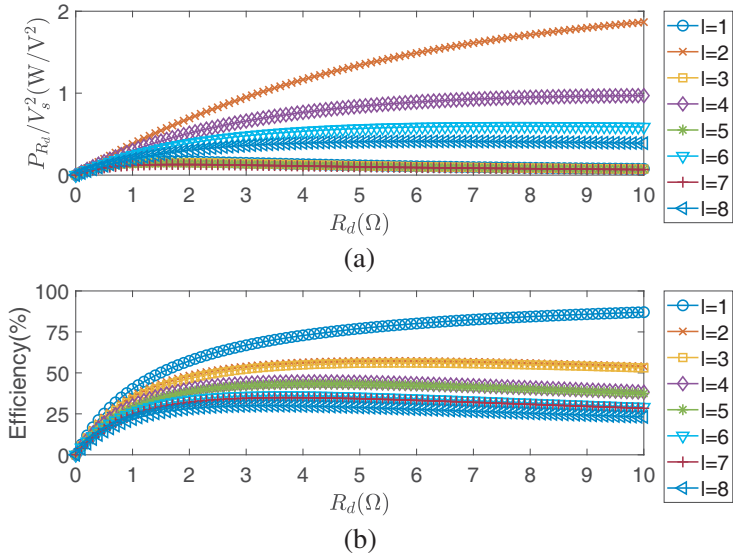

Figure 8. Values of (a) the power delivered to R_d and (b) the efficiency (%), versus R_d for different positions of the receiver l for an array terminated with $R_{eq,\infty}$.

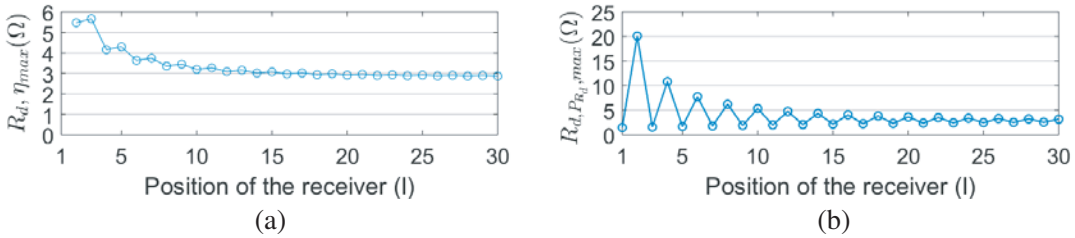

Figure 9. Value of (a) $R_{d,\eta_{R_d}\max(R_{eq,N-l}=R_{eq,\infty})}$ versus the position of the receiver and (b) $R_{d,P_{R_d}\max(R_{eq,N-l}=R_{eq,\infty})}$ versus the position of the receiver.

It can be noticed that for an increasing number of resonators both $R_{d,\eta_{\max}}$ and $R_{d,P_{R_d}\max}$ tend to a constant value; in fact,

$$\lim_{l\to\infty} R_{d,P_{R_d}\max(R_{eq,N-l}=R_{eq,\infty})} = \sqrt{4(\omega_0 M)^2 + R^2} = \lim_{l\to\infty} R_{d,\eta_{R_d}\max(R_{eq,N-l}=R_{eq,\infty})} \tag{22}$$

which for a very low loss line ($R \ll \omega_0 M$) tends to $2\omega_0 M$. In the plots of Figs. 9(a) and 9(b), Eq. (22) is equal to 2.87 Ω; $R_{d,\eta_{\max}}$ converges to this value quicker than $R_{d,P_{R_d}\max}$ and with smaller oscillations.

By substituting Eqs. (20) and (21) in Eqs. (18) and (17), respectively, the maximum efficiency and power delivered to the receiver can be obtained; they are plotted versus r and for different positions of the receiver over an array terminated with $R_{eq,\infty}$ (see Figs. 10(a) and 10(b), respectively).

Figure 10(a) shows that the maximum power delivered to a receiver decreases with the increase of r (meaning higher losses in the array); for the same value of r, higher values are found for even receiver positions (l = 2, 4, 6 and 8) rather than for odd positions (l = 1, 3, 5 and 7). Similarly, as Fig. 10(b) shows, the maximum efficiency decreases with the increase of r and when the receiver gets far away from the power source. It can also be noted that the maximum power and maximum efficiency shown in Figs. 10(a) and 10(b) are lower than the ones in Figs. 6(a) and 6(b), since now we are considering that the resonator array has other cells after the cell under the receiver, which leads to extra losses.

All the previous considerations on the power delivered to R_d, P_{R_d}, were made considering a voltage source with a constant RMS value V_s. If the RMS value V_s is variable, Eq. (17) can be used to determine the value of V_s needed to keep P_{R_d} constant regardless of the position l of the receiver, as shown in Fig. 11.

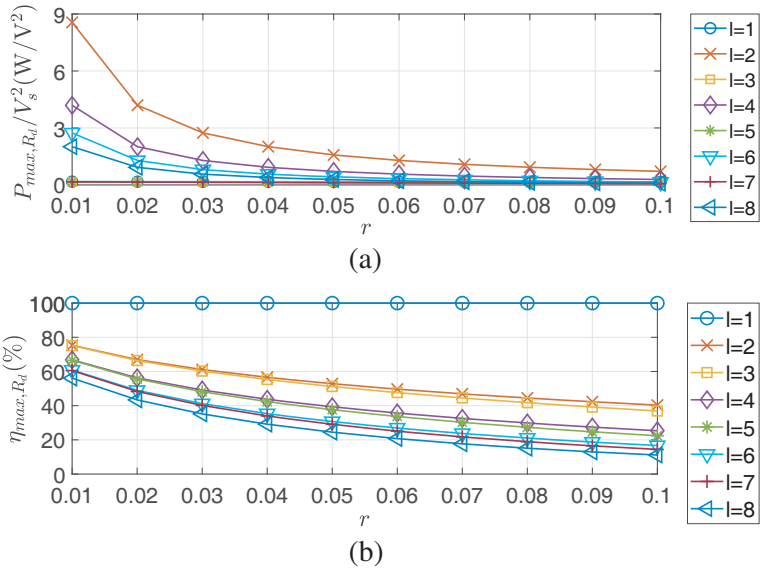

Figure 10. Values of (a) the maximum power delivered to a receiver R_d and (b) maximum efficiency versus r for different positions of the receiver l.

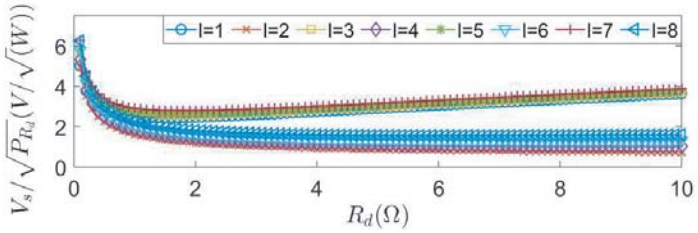

Figure 11. RMS value of the voltage source V_s for a fixed power P_{R_d} versus R_d and for different positions of the receiver l (the array is terminated with $R_{eq,\infty}$)

3.4. Power Transmitted Considering the Losses in the Receiver

In the previous section, the analysis of the power delivered to a receiver and the IPT system efficiency has been made simpler representing the receiver with an impedance $\hat{Z}_d$ that takes into account also the receiver losses (due to its intrinsic AC resistance R_r) and a load R_{load} connected to it (see Figs. 2(a) and (b)). The power delivered to R_{load} is then given by:

$$P_{R_{load}} = I_r^2 R_{load} \tag{23}$$

where I_r is the RMS value of the current of the receiver, which can be written in terms of the RMS value of the current I_l in the lth resonator of the array according to the circuit represented in Fig. 2(a). Assuming that the resonant frequency of the receiver is the same than that of the cells of the array, as seen in [9, 20], I_r is given by:

$$I_r = \frac{\omega_0 M_{r,l} I_l}{R_r + R_{load}}. \tag{24}$$

$M_{r;l}$ being the mutual inductance between the receiver and the cell beneath it (lth cell), as Fig. 2(a) shows. The power absorbed by R_d is $P_{R_d} = I_l^2 R_d$, where R_d can be calculated as [9]:

$$R_d = \frac{(\omega_0 M_{r,l})^2}{R_r + R_{load}}. \tag{25}$$

Using Eqs. (23) and (24) we can write

$$\frac{P_{R_{load}}}{P_{R_d}} = \frac{R_{load}}{R_r + R_{load}}. \tag{26}$$

According to Eq. (26), the power delivered to the load can be maximized by having R_{load} much larger than R_r. For Eq. (25) this could imply a lower value of R_d if $M_{r,l}$ is not high enough. Then, for a given value of R_d, in order to suppress the effect of R_r, both $M_{r,l}$ and R_{load} should be made as large as possible. Under this condition the power and efficiency can thus be calculated with Eqs. (15), (16), (17) and (18), as $P_{R_{load}}/P_{R_d} \simeq 1$. Otherwise, the power delivered to R_{load} can be obtained by multiplying Eq. (26) by P_{R_d}.

4. EXPERIMENTAL VERIFICATION

4.1. Experimental Setup

The theoretical analysis presented in the previous section was verified experimentally using the resonator array built in laboratory used in [14, 21]. The circuital parameters of each resonator (self-inductance, intrinsic AC resistance and added capacitance) and its resonant frequency were measured using an Agilent 4396B 100 kHz–1.8 GHz Vector Network Analyser (VNA) and were reported in [14, 21].

As in [14, 21], the power supply used in the experimental setup consisted of a full-bridge inverter (a Fairchild Semiconductor FSB44104A) supplied by a AIM-TTI Instruments QPX1200SP 1200W DC Power Supply controlled by an Arduino Due microprocessor. The input current was measured with a 500 MHz Agilent Infiniium 54825A digital oscilloscope and a Tektronix TCP305 DC to 50 MHz current probe. The voltages were measured using a TESTEC TT-SI 9002 voltage differential probe connected to the same oscilloscope.

The RMS value of the voltage source V_s used for calculations was experimentally determined as in [14, 22]:

$$V_s = V_{s1} = \frac{4}{\pi\sqrt{2}} V_{sq} \tag{27}$$

where V_{s1} is the RMS of the fundamental component of the inverter output square-wave v_{in}, and V_{sq} is the measured amplitude value of the square wave, whose duty cycle is assumed to be 0.5. Even if the voltage source has a waveform different from the sinusoidal one (square wave in the case considered), the purely sinusoidal approach, used for the circuit of Fig. 1, is still valid when the system is in the resonance condition. In fact, as reported in [22] and explained in [23], a resonant circuit acts as a filter for the frequencies different than the one of resonance. As a result, the current and voltage resulting waves in the circuit are sinusoidal.

4.2. Power and Efficiency

The measured values for the power transmitted and efficiency were obtained by measuring the input power ($P_{in,\mathrm{exp}}$) and the power delivered to a load connected to the last cell ($P_{R_T,\mathrm{exp}}$) or a receiver ($P_{R_{load},\mathrm{exp}}$). The input power was determined by calculating the average value over a period of the product of the instantaneous voltage $v_{in}(t)$ and current $i_{in}(t)$ measured at the terminals of the inverter. $P_{in,\mathrm{exp}}$ and its average value in a period were calculated with the mathematical functions of the oscilloscope, as in [12]. The power delivered to a given load was calculated as the ratio of the square RMS value of the voltage measured at the load terminals (V_T or V_{load}) to the load (R_T or R_{load}):

$$P_{R_T,\mathrm{exp}} = V_T^2/R_T;\ P_{R_{load},\mathrm{exp}} = V_{load}^2/R_{load}. \tag{28}$$

We can then calculate the experimental value of the system efficiency as

$$\eta_{R_T,\mathrm{exp}} = P_{R_T,\mathrm{exp}}/P_{in,\mathrm{exp}};\ \eta_{R_{load},\mathrm{exp}} = P_{R_{load},\mathrm{exp}}/P_{in}. \tag{29}$$

An example of the waveforms of $v_{in}(t)$, $i_{in}(t)$ and the voltage at the terminals of the termination resistance $v_T(t)$ is shown in Fig. 12. The voltage $v_T(t)$ leads the input voltage $v_{in}(t)$ by 90 degrees. This happens because the current in the 6th resonator leads the first resonator current by 90 degrees, as seen in Subsection 3.1.

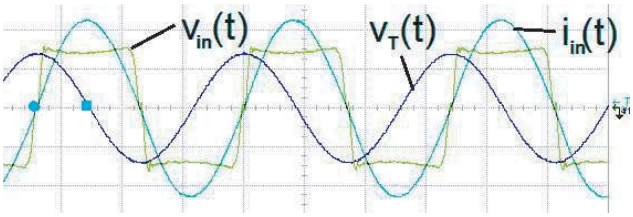

Figure 12. Example of the waveforms of $v_{in}(t)$, $i_{in}(t)$ and of $v_T(t)$ for $R_T = 1.5\,\Omega$, $v_T(t)$ measured with the oscilloscope. Horizontal scale: $2\,\mu$s/div. Vertical scale $10\,$V/div and $5\,$A/div.

4.2.1. Power Delivered to a Load or a Receiver over the Last Cell and Efficiency

The power delivered to a load or a receiver over the last cell and the efficiency of the system were respectively calculated with Eqs. (8) and (9) and compared to those obtained from measurements with Eqs. (28) and (29). They are plotted versus R_T in Fig. 13 (for $V_s = 4.9\,$V and an array with 6 resonators) and versus the number of resonators N in Fig. 14 (for $V_s = 12.1\,$V and an array terminated with $R_T = 1.5\Omega$).

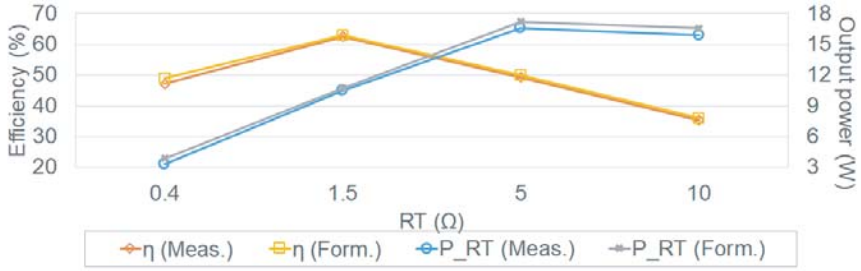

Figure 13. Comparison between the values of P_{R_T} and η_{R_T} obtained with measurements (using Eqs. (28) and (29)) and the developed formulas (8) and (9) versus R_T for a 6-resonator array.

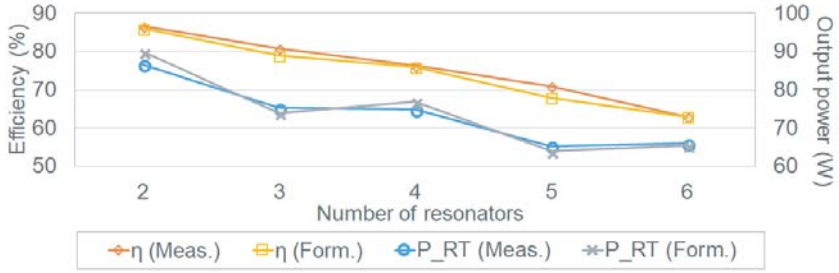

Figure 14. Comparison between the values of P_{R_T} and η_{R_T} obtained with measurements (using Eqs. (28) and (29)) and the developed formulas (8) and (9) versus the number of resonators for a termination resistance $R_T = 1.5\,\Omega$.

For the considered array configuration, the values of R_T that yield the maximum efficiency and maximum power transfer are found as $R_{T,\eta_{\max}} = 1.44\,\Omega$ and $R_{T,P_{R_T,\max}} = 6.4\,\Omega$ using Eqs. (10) and (11), respectively.

It can be noticed from Fig. 13 that the highest value of the efficiency η_{R_T} is obtained when the value R_T is closest to the value of $R_{T,\eta_{\max}}$; the same is found for the power delivered to a load P_{R_T}: the maximum power transfer occurs when the value of R_T is closest to $R_{T,P_{R_T,\max}}$. Thus, depending on the type of application for which the array is designed (maximum efficiency or maximum power transfer), there exist different optimal values of R_T.

Moreover, we can notice from Fig. 14 that for a given value of $R_T = 1.5\,\Omega$ both η_{R_T} and P_{R_T} decrease with the number of resonators N, the former almost linearly. The efficiency is between 63% and 88% and the delivered power between 65 W and 90 W; these power levels are higher than what usually reported in literature for IPT systems with resonator arrays [7, 15, 24].

4.2.2. Power Delivered to a Receiver over the lth Cell and Efficiency

Figure 15 shows the experimental setup used to measure the power delivered to a receiver over the array and the efficiency of the IPT system. For simplicity, the receiver is identical to the stranded-wire resonators (thus $R_r = R$ in Eqs. (25) and (26)) and a load $R_{load} = 5\,\Omega$ is connected to it.

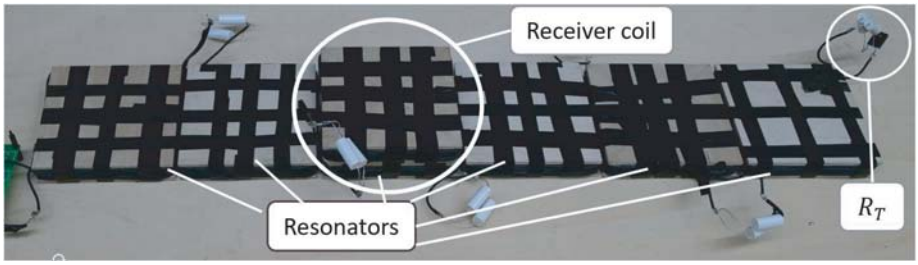

Figure 15. Experimental setup used to measure the power delivered to a receiver over the array and the efficiency of the IPT system.

The array is fed with $V_s = 4.9\,\text{V}$ and terminated with $R_T = 1.5\,\Omega$; the measured mutual inductance between each array cell and the receiver (for a distance of 1 cm) is $M_{r,l} = 4.8\,\mu\text{H}$, which yields $R_d = 3.8\,\Omega$ from Eq. (25). Being the termination impedance close to that perfectly terminating the array ($R_{eq,\infty} = 1.38\,\Omega$), the power delivered to the load and the efficiency obtained with measurements using Eqs. (28) and (29) are compared to those calculated with Eqs. (17) and (18) multiplied by the term on the right of Eq. (26) (equal to 0.98 in this example):

$$P_{R_{load}} = \frac{P_{R_d} R_{load}}{R_r + R_{load}}; \quad \eta_{R_{load}} = \frac{\eta_{R_d} R_{load}}{R_r + R_{load}}. \tag{30}$$

The results of the comparison are shown in Fig. 16 and show a good agreement, thus validating all the formulas developed in Section 3. As it was observed in Figs. 8(a) and 8(b), the delivered power depends on the position of the receiver and the values are higher for even positions, while the efficiency decreases as the receiver moves far away from the power source.

Eventually, we can study the relation between the distance of the receiver from the array and the power transfer and efficiency for different receiver positions. Besides the distance of 1 cm from the array,

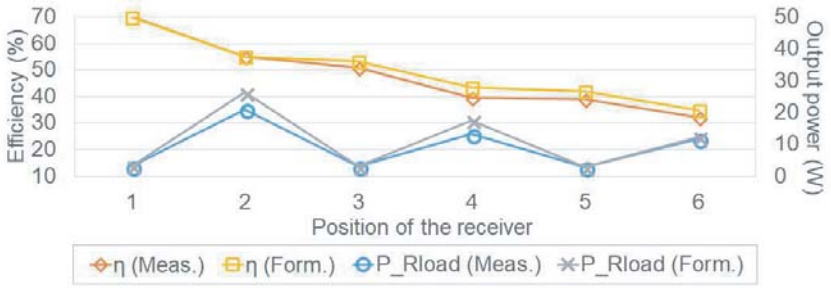

Figure 16. Comparison between the values of $P_{R_{load}}$ and $\eta_{R_{load}}$ obtained with measurements (using Eq. (28) and (29)) and the developed formulas ((17), (18) and (26)) versus the receiver position for a 6-resonator array terminated with $R_T = 1.5\,\Omega$ and a receiver connected to a load $R_{load} = 5\,\Omega$ and distant 1 cm from the array.

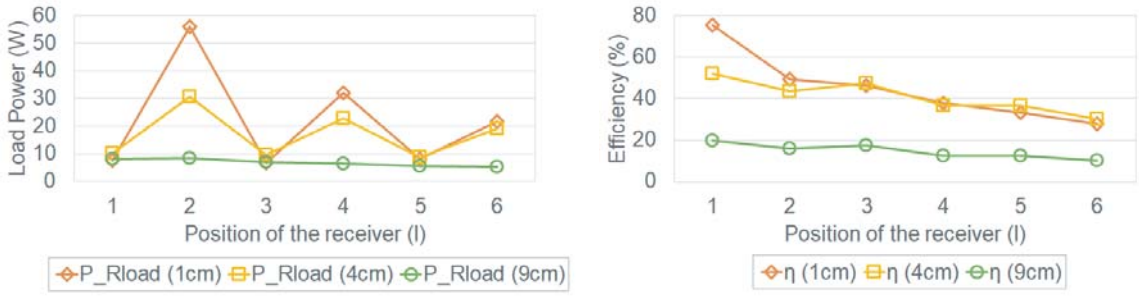

Figure 17. (a) Power delivered to $R_{load} = 3.3\,\Omega$ determined with Eq. (28) and (b) efficiency of the system determined with Eq. (29) versus the position of the receiver and for three different distances between the receiver and the array.

distances of 4 cm and 9 cm were considered, which correspond to mutual inductance values between the receiver and the cell below it of $M_{r,l} = 2.7\,\mu H$ and $M_{r,l} = 1.2\,\mu H$, respectively. Considering a load $R_{load} = 3.33\,\Omega$ connected to the receiver, Eq. (25) yields values of R_d of $5.7\,\Omega$, $1.8\,\Omega$ and $0.4\,\Omega$ for distances of 1, 4 and 9 cm, respectively. The power delivered to R_{load} and efficiency determined with Eqs. (28) and (29) are shown in Fig. 17 versus the receiver position for the three different distances between the receiver and the array, considering a voltage source with a constant RMS value. It can be noticed from Fig. 17 that the efficiency decreases for increasing distances of the receiver from the power source, while the power transmitted to the load oscillates. Moreover, the power delivered to R_{load} decreases as the distance from the receiver to the cell of the array under it increases, when it is in an even position (2, 4 and 6). However, when the receiver is on an even position (1, 3 and 5) the increase in the distance from the receiver to the cell under it does not change the power transmitted to the load significantly. Moreover, the variation of $P_{R_{load}}$ as the receiver moves away from the power source decreases, and $P_{R_{load}}$ becomes approximately constant regardless of the position of the receiver when the distance is 9 cm.

5. CONCLUSIONS

In this paper, by determining the inverse of the impedance matrix, which has the form of a tridiagonal matrix, the analytical expression of the current in each resonator can be obtained and thus both the power delivered to a load terminating the array or to a receiver over the array and the efficiency of the IPT system can be determined.

Using these expressions, the values of the delivered power and efficiency for different conditions and parameters of the system are obtained for various configurations of the IPT system, thus allowing a better understanding of the behaviour of an IPT system which uses a resonator array. Moreover, using the developed expressions one can determine analytically the maximum possible values of power transferred and efficiency for given conditions of the IPT system and also which conditions and system parameters lead to maximum power transfer and efficiency.

It is found that the values of the currents in the array resonators oscillate from the first to the last resonator when the array is not perfectly terminated and that the peaks occur on even or odd resonators depending on the termination impedance value. Moreover, the values of the maximum power transfer and maximum efficiency depend on the electrical parameters of the array, value of the impedance of the termination load or the receiver, position of the receiver, number of resonators, etc. It is found that the transferred power has opposite behaviour for odd or even numbers of resonators N or for the difference between the number of resonators and position of the receiver, $N - l$. It is shown that there exist different optimal values of the termination impedance yielding maximum efficiency or maximum power transfer; thus, depending on the application desired, the expressions can be used to optimize the IPT system regarding maximum power transfer, maximum efficiency or constant power delivered.

The expressions and formulas developed were validated by measurements on an IPT system

composed of an array of stranded wire resonators fed by a power inverter, thus showing their practical applicability for the design of IPT systems with resonator arrays. The behaviour of the system can be easily predicted for given electrical parameters of the system and different positions of the receiver thus saving time in comparison to numerical calculations or simulations. Finally, the utilization of a system capable of delivering up to 90 W of power shows that these arrays can also be used for applications that require a higher amount of power (e.g., charging or powering small home devices).

ACKNOWLEDGMENT

H. Albuquerque acknowledges financial assistance by the Centre for Mathematics of the University of Coimbra — UID/MAT/00324/2013, funded by the Portuguese Government through FCT/MEC and co-funded by the European Regional Development Fund through the Partnership Agreement PT2020.

REFERENCES

1. Shinohara, N., "The wireless power transmission: Inductive coupling, radio wave, and resonance coupling," *Wiley Interdisciplinary Rev.: Energy and Environment*, Vol. 1, No. 3, 337–346, 2012.
2. Casanova, J. J., Z. N. Low, and J. Lin, "A loosely coupled planar wireless power system for multiple receivers," *IEEE Trans. on Ind. Electron.*, Vol. 56, No. 8, 3060–3068, Aug. 2009.
3. Ahmad, A., M. S. Alam, and R. Chabaan, "A comprehensive review of wireless charging technologies for electric vehicles," *IEEE Trans. Transport. Electrific.*, Vol. 4, No. 1, 38–63, Mar. 2018.
4. Ranum, B. T., N. W. D. E. Rahayu, and A. Munir, "Development of wireless power transfer receiver for mobile device charging," *The 2nd IEEE Conf. on Power Eng. and Renewable Energy (ICPERE) 2014*, 48–51, Dec. 2014.
5. Xue, R. F., K. W. Cheng, and M. Je, "High-efficiency wireless power transfer for biomedical implants by optimal resonant load transformation," *IEEE Trans. Circuits Syst. I, Reg. Papers*, Vol. 60, No. 4, 867–874, Apr. 2013.
6. Liu, Z., Z. Chen, Y. Guo, and Y. Yu, "A novel multi-coil magnetically-coupled resonance array for wireless power transfer system," *2016 IEEE Wireless Power Transfer Conf (WPTC)*, 1–3, May 2016.
7. Zhong, W., C. K. Lee, and S. Y. R. Hui, "General analysis on the use of Tesla's resonators in domino forms for wireless power transfer," *IEEE Trans. Ind. Electron.*, Vol. 60, No. 1, 261–270, Jan. 2013.
8. Zhang, X., S. L. Ho, and W. N. Fu, "Quantitative design and analysis of relay resonators in wireless power transfer system," *IEEE Trans. Magn.*, Vol. 48, No. 11, 4026–4029, Nov. 2012.
9. Puccetti, G., C. J. Stevens, U. Reggiani, and L. Sandrolini, "Experimental and numerical investigation of termination impedance effects in wireless power transfer via metamaterial," *Energies*, Vol. 8, No. 3, 1882–1895, 2015.
10. Monti, G., L. Corchia, L. Tarricone, and M. Mongiardo, "A network approach for wireless resonant energy links using relay resonators," *IEEE Trans. Microw. Theory Techn.*, Vol. 64, No. 10, 3271–3279, Oct. 2016.
11. Alberto, J., U. Reggiani, and L. Sandrolini, "Circuit model of a resonator array for a WPT system by means of a continued fraction," *Proc. 2016 IEEE 2nd Int. Forum on Research and Technol. for Society and Ind. Leveraging a Better Tomorrow (RTSI)*, 1–6, Bologna, Italy, Sept. 2016.
12. Alberto, J., G. Puccetti, G. Grandi, U. Reggiani, and L. Sandrolini, "Experimental study on the termination impedance effects of a resonator array for inductive power transfer in the hundred kHz range," *Proc. 2015 IEEE Wireless Power Transfer Conf. (WPTC 2015)*, 1–4, Boulder, CO, USA, May 2015.
13. Alberto, J., U. Reggiani, and L. Sandrolini, "Magnetic near field from an inductive power transfer system using an array of coupled resonators," *2016 Asia-Pacific Int. Symp. on Electromagn. Compat. (APEMC)*, Vol. 01, 876–879, May 2016.

14. Alberto, J., U. Reggiani, L. Sandrolini, and H. Albuquerque, "Fast calculation and analysis of the equivalent impedance of a wireless power transfer system using an array of magnetically coupled resonators," *Progress In Electromagnetics Research B*, Vol. 80, 101–112, 2018.
15. Stevens, C. J., "Magnetoinductive waves and wireless power transfer," *IEEE Trans. Power Electron.*, Vol. 30, No. 11, 6182–6190, Nov. 2015.
16. Zhang, Y., Z. Zhao, and K. Chen, "Frequency-splitting analysis of four-coil resonant wireless power transfer," *IEEE Trans. Ind. Appl.*, Vol. 50, No. 4, 2436–2445, Jul. 2014.
17. Solymar, L. and E. Shamonina, *Waves in Metamaterials*, OUP Oxford, 2009.
18. Parise, M. and G. Antonini, "On the inductive coupling between two parallel thin-wire circular loop antennas," *IEEE Trans. on Electromagn. Compat.*, Vol. 60, No. 6, 1865–1872, Dec. 2018.
19. Fonseca, C. D. and J. Petronilho, "Explicit inverse of a tridiagonal k-toeplitz matrix," *Numerische Mathematik*, Vol. 100, No. 3, 457–482, 2005.
20. Wang, C.-S., O. H. Stielau, and G. A. Covic, "Design considerations for a contactless electric vehicle battery charger," *IEEE Trans. Ind. Electron.*, Vol. 52, No. 5, 1308–1314, Oct. 2005.
21. Alberto, J., U. Reggiani, and L. Sandrolini, "Study of the conducted emissions of an ipt system composed of an array of magnetically coupled resonators," *Proc. 2017 IEEE Int. Symp. on Electromagn. Compat. Signal/Power Integrity (EMCSI)*, 623–628, Aug. 2017.
22. Kazimierczuk, M. K., "Class d voltage-switching mosfet power amplifier," *IEE Proceedings B-Electric Power Applications*, Vol. 138, No. 6, 285–296, IET, 1991.
23. Kazimierczuk, M. and D. Czarkowski, *Resonant Power Converters*, Wiley, 2012.
24. Zhong, W. X., C. K. Lee, and S. Y. Hui, "Wireless power domino-resonator systems with noncoaxial axes and circular structures," *IEEE Trans. Power Electron.*, Vol. 27, No. 11, 4750–4762, Nov. 2012.